IUG Journal of Natural Studies
Peer-reviewed Journal of Islamic University-Gaza

ISSN 2409-4587

IUGNS
Vol 25, No 1, 2017, pp 74-81

Received on (24-08-2016) Accepted on (07-11-2016)

Spatio-Temporal Modeling of Sodium Adsorption Ratio (SAR) in Groundwater: The Case of Gaza Strip

Esam Mahdi[1],*

[1]Department of Mathematics Faculty of Science, Islamic University of Gaza, Gaza Strip, Palestine

*** Corresponding author**
e-mail address: emahdi@iugaza.edu.ps

Abstract

In this paper we consider the geostatistical analysis methods to explain the dependency of the Sodium Adsorption Ratio (SAR) in the groundwater datasets throughout the Gaza Strip. The spatio-temporal ordinary kriging is used to estimate the SAR values for the period 2001 to 2009. The results show positive increasing trend in the SAR values over the time that may seriously deteriorate the quality of the irrigation and drinking water in the Gaza Strip.

Keywords:
Geostatistical analysis, Spatio-temporal models, Variogram, Kriging, Sodium adsorption ratio (SAR), and Gaza Strip.

1. Introduction:

Spatio-temporal statistical models arise when data is collected across space as well as time domain. The most important feature that distinguishes spatio-temporal analysis from classical statistical analysis is that spatio-temporal model uses the spatial coordinates (locations), at which the observations form a time series, to model statistical dependence among data, rather than assuming that the data is independent.

Over the years, numerous progress has been made in building spatial geostatistical models in several environmental phenomena ignoring the possibility of the existence of temporal structure within such phenomena. For instant, Omran (2012) proposed a spatial geostatistical model to evaluate and map groundwater quality for irrigation in Darb El-Arbaein, in Southwestern Desert of Egypt; Moasheri, but he did not consider the possible existence of the temporal dependency in such a data. Moreover, Honarbakhsh and Farsani (2013) compared the Artificial Neural Network (ANN) to the Geostatistics methods in estimating the distribution of the Sodium Adsorption Ratio (SAR) in groundwater data in Birjand Plain, Iran using the spatial locations to model the dependency, ignoring the effect of the time factor. On the contrary to spatial models, there has not been enough implementations to spatio-temporal theory in modeling and describing spatio-temporal variation in terms of water suitability for irrigation.

In this paper, we propose a space-time[1] model that may help in estimating the hazard effect from the high level of the SAR values in the groundwater throughout Gaza Strip. We hope that the decision-makers, water-resource managers, and private users

[1] Space-time terminology is used when data is measured in a space of two dimension over a period of time, whereas spatio-temporal is used when data is measured in n-dimensional space over a period of time.

in Gaza Strip will benefit from this research in preparing strategic plans in order to protect water supplies based on the results reported in this article.

The plan of the paper is as follows. Section 2 presents the statistical methodology followed to model the SAR of irrigation water in space and time domain. Section 3 describes the study area together with the dataset motivating this paper. The geostatistical results are reported in detail in Section 4. The paper ends with some final conclusions and discussion of the results.

1. Statistical models for space-time SAR of irrigation water:

Consider the space-time hierarchical stochastic processes for the SAR of irrigation water $\{Z(s,t): (s,t) \in \boldsymbol{\mathcal{S}} \times \boldsymbol{\mathcal{T}}\}$ that are observed in a continuous geospatial domain $\boldsymbol{\mathcal{S}} \subseteq \mathbb{R}^{\mathbf{2}}$ and a discrete-time index set $\boldsymbol{\mathcal{T}} \subseteq \mathbb{Z}$ and modeled as

$$Z(s,t) = \mu(s,t) + \varepsilon(s,t), \quad s \in \boldsymbol{\mathcal{S}}, \ t \in \boldsymbol{\mathcal{T}}, \tag{1}$$

where $\mu(s,t)$ defines a spatially varying deterministic trend over longer time scales, which is usually modelled as a linear function of known p-predictors $\sum_{j=0}^{p} \beta_j X_j(s,t)$ with $X_j(s,t)$ the known spatial temporal p-regressors and β_j unknown regression coefficients, usually containing an intercept for which $X_0(s,t) = 1$ and the random effect $\varepsilon(s,t)$ can be rewritten as $\zeta(s,t) + e(s,t)$ where $e(s,t)$ is a zero-mean white noise process whereas $\zeta(s,t)$ is a mean-zero space-time process (Jones and Zhang (1997) and Cressie and Wikle (2011, Ch.6)).

Suppose that we wish to predict the unobserved value $Z(s_0, t_0)$ based on the values of the observed data of size n. This would be done by kriging interpolation methods which give the best linear unbiased prediction (Isaaks and Srivastava 1989, p.289). Ordinary Kriging (OK) and lognormal Kriging were used to produce the spatial patterns of heavy metals and disjunctive Kriging was applied to quantify the probability of heavy metal concentrations higher than their guide values (Liu,Wu, and Xu 2005). Geostatistical methods, Kriging and Co-Kriging, were applied to estimate the sodium adsorption ratio (SAR) in a 3,375 ha agricultural field (Pozdnyakova and Zhang 1999).

Kriging predictor, $\hat{Z}(s_0, t_0)$ takes the form of a linear combination of the data as follows

$$\hat{Z}(s_0, t_0) = \sum_{i=1}^{m} \sum_{j=1}^{n_i} \omega_{ij}(s_0, t_0) Z(s_i, t_{ij}), \tag{2}$$

where $s_i, i = 1,2,\ldots,m$ is the i^{th} spatial location; $t_{ij}, j = 1,2,\ldots,n_i$ are the n_i^{th} temporal corresponding to s_i; the weights $\omega_{ij}(s_0, t_0)$ can be estimated by minimizing the mean squared prediction error subject to $E[Z(s,t)] = \mu(s,t)$; and $n_1 + n_2 + \cdots + n_m = n$.

The model in Equation 2 is commonly assumed to be isotropic[2] and intrinsically stationary; that is,

$$E[Z(s,t) - Z(\tilde{s},\tilde{t})] = 0, \qquad Var[Z(s,t) - Z(\tilde{s},\tilde{t})] = 2\gamma(h,u), \tag{3}$$

or equivalently (under the constant mean assumption) $2\gamma(h,u) = E[Z(s,t) - Z(\tilde{s},\tilde{t})]^2$; where $2\gamma(h,u)$ is referred to *Space-time Variogram*; h is the spatial Euclidian distance between the two points s and $\tilde{s}$; and u is the temporal distance between the two times t and $\tilde{t}$. The estimate of the space-time variogram is needed in order to derive the weights in Equation 3.

In this article, the word space-time variogram will be used synonymously with space-time semivariogram, where $\gamma(h,u)$ is referred to *Space-time Semivariogram*[3]. The stationary autocovariance function of this model is

$$C(h,u) = Cov(Z(s,t), Z(s+h, t+u)). \tag{4}$$

In general, it is not easy to estimate this function. In this respect, some space-time covariance models together with bounded space-time variograms, $\gamma(h,u) = C(0,0) - C(h,u)$, were presented in order to simplify the model assumptions.

A crucial notion for a valid stationary covariance functions is that of nonnegative definite for all finite collections of space-time coordinates. In general, it can be quite difficult to check whether a space-time covariance function is positive definite, so that the parametric space-time covariance models have been constructed based on the purely spatial covariance and

[2] A process is isotropic if the invariance structure holds under rotation and translation.
[3] $2\gamma(h,0)$ represents the spatial variogram whereas $2\gamma(0,u)$ represents the temporal variogram.

purely temporal covariance. The common parametric space-time covariance models used in literature are:

The product (Separable) covariance model (Cesare, Myers, and Posa 1997), which is defined in terms of the product of the spatial and temporal terms, so that the space-time covariance has a temporal component and a spatial component that do not interact:

$$C_{prod}(h,u) = C_s(h)C_t(u), \tag{5}$$

and the corresponding space-time variogram is given by

$$\gamma_{prod}(h,u) = C_{prod}[\gamma_s(h) + \gamma_t(u) - \gamma_s(h)\gamma_t(u)], \tag{6}$$

where $\gamma_s(h)$ and $\gamma_t(u)$ are the standardized intrinsically stationary spatial and temporal variograms respectively with a global sill C_{prod}. It is worth noted that this model is the most common one used in geostatistical space-time data.

The linear covariance model (Rouhani and Hall 1989) which produced by adding uncorrelated spatial and temporal covariances together as follows

$$C_{sum}(h,u) = C_s(h)+C_t(u), \tag{7}$$

The problem with this covariance model is that it is not always positive semidefinite and in many cases it has unsatisfactory results for optimal prediction (Myers and Journel 1990; Rouhani and Myers 1990).

The product-sum covariance model (Cesare, Myers, and Posa 2001), which is a linear combination of the product and the linear of spatial and temporal terms, obtained in the following formula

$$C_{ps}(h,u) = kC_s(h)C_t(u) + C_s(h)+C_t(u), \tag{8}$$

with $k > 0$. The corresponding variogram can be written as

$$\gamma_{ps}(h,u) = (1 + kC_t)\gamma_s(h) + (1 + kC_s)\gamma_t(u) - k\gamma_s(h)\gamma_t(u), \tag{9}$$

where C_s is the partial sill of the spatial variogram $\gamma_s(h)$; C_t is the partial sill of the temporal variogram $\gamma_t(u)$; and C_{ps} is the global sill of $\gamma_{ps}(h,u)$ with $C_{ps} = kC_sC_t + C_s + C_t$.

The generalized product-sum covariance model proposed by Iaco, Myers, and Posa (2001) is

$$C_{gps}(h,u) = k_1C_s(h)C_t(u) + k_2C_s(h)+k_3C_t(u), \tag{10}$$

for some $k_1 > 0$, $k_2 \geq 0, k_3 \geq 0$. The corresponding variogram is given by

$$\gamma_{gps}(h,u) = (k_2 + k_1C_t)\gamma_s(h) + (k_3 + k_1C_s)\gamma_t(u) - k_1\gamma_s(h)\gamma_t(u), \tag{11}$$

where C_s is the partial sill of $\gamma_s(h)$, C_t is the partial sill $\gamma_t(u)$, and C_{gps} is the global sill of $\gamma_{gps}(h,u)$.

The metric covariance model (Dimitrakopoulos and Luo 1994), assumes that spatial and temporal covariances are equal to a joint covariance model C_{joint} with an anisotropy correction parameter, κ. The metric covariance model is

$$C_m(h,u) = C_{joint}(\sqrt{h^2 + \kappa^2u^2}), \tag{12}$$

and its associated variogram including the joint variogram γ_{joint} with some nugget effect is

$$\gamma_m(h,u) = \gamma_{joint}(\sqrt{h^2 + \kappa^2u^2}), \tag{13}$$

The sum-metric covariance model (Bilonick 1988), is defined as a combination of spatial, temporal and metric model as follows

$$C_{sm}(h,u) = C_s(h) + C_t(u) + C_{joint}(\sqrt{h^2 + \kappa^2u^2}), \tag{14}$$

and the associated variogram with a joint variogram is

$$\gamma_{sm}(h,u) = \gamma_s(h) + \gamma_t(u) + \gamma_{joint}(\sqrt{h^2 + \kappa^2u^2}), \tag{15}$$

where $\gamma_s(h), \gamma_t(u)$ and γ_{joint} are spatial, temporal and joint variograms respectively with separate nugget-effects.

It should be noted that the above mentioned purely spatial, purely temporal and space-time covariance and variogram models need not necessarily exhibit the same structure.

The moment spatial variogram estimator that was originally introduced by Matheron (1962, 1963b,a) can be modified to estimate the separate spatial and temporal variograms in space-time data, respectively, as follows

$$\hat{\gamma}(h) = \frac{1}{N(t)}\sum_{t}\frac{1}{2|N(h)|}\sum_{(s_i,s_j)\in N(h)}\left(Z(s_i,t)-Z(s_j,t)\right)^2 \qquad (16)$$

$$\hat{\gamma}(u) = \frac{1}{N(s)}\sum_{s}\frac{1}{2|N(u)|}\sum_{(t_i,t)\in N(u)}\left(Z(s,t_i)-Z(s,t_j)\right)^2 \qquad (17)$$

Where $|N(h)|$ and $|N(u)|$ stand for the number of distinct pairs in $N(h)$ and $N(u)$, which are the set formed by those locations and times that are a distance h and u apart respectively.

The empirical space-time variogram is obtained by a straightforward extension of the previous empirical variograms. The moment space-time estimator for stationary and isotropic processes is

$$\hat{\gamma}(h,u) = \frac{1}{2|N_{uh}|}\sum_{((s_i,s_j);(t_i,t_j))\in N_{uh}}\left(Z(s_i,t_i)-Z(s_j,t_j)\right)^2 \qquad (18)$$

where $|N_{uh}|$ stands for the number of distinct pairs in N_{sh}, which is the set formed by those locations and times that are a distance $h\in\mathbb{R}^{\boldsymbol{d}}$ and $u\in\mathbb{R}$ apart. Generally we use a tolerance region for the lag distance h and the lag time u such as: $\|h\|-\Delta_s\leq\|s_i-s_j\|\leq\|h\|+\Delta_s$ and $|u|-\Delta_t\leq|t_i-t_j|\leq|u|+\Delta_t$, where $\|.\|$and $|.|$ referred to Euclidean norm in $\mathbb{R}^{\boldsymbol{d}}$and $\mathbb{R}$ respectively (Cressie 1993).

One crucial assumption of the variogram is conditional negative-definite, here defined

$$\sum_{i=1}^{n}\sum_{j=1}^{n} a_i a_j 2\gamma((s_i,t_i),(s_j,t_j))\leq 0, \qquad (19)$$

for any finite number of space-time locations $(s_1,t_1),\cdots,(s_n,t_n)$and real numbers $a_1,\cdots,a_n$ satisfying $\sum_{i=1}^{n} a_i=0$ (Dunn 1983).

In many situations, the empirical variogram based on the usual method-of-moments of a sample is not guaranteed to be conditionally negative-definite (Cressie 1993, p. 69). The common valid variogram models used in spatial statistics, the linear, exponential, spherical, wave, and the Gaussian models are briefly presented in this section and defined as follows: (the parameters $\theta=(c_0,c,r)$ are the ***nugget*** effect[4], the ***partial sill***[5], and the ***range***[6] respectively).

The spatial linear variogram model

$$\gamma(h;\theta)=\begin{cases} c_0+c(h/r), & if\ h<r;\\ c_0+c, & otherwise.\end{cases} \qquad (20)$$

The spatial exponential variogram model

$$\gamma(h;\theta)=c_0+c(1-\exp(-3h/r)). \qquad (21)$$

The spatial spherical variogram model

$$\gamma(h;\theta)=\begin{cases} c_0+c(1.5(h/r)-0.5(h/r)^3), & if\ h<r;\\ c_0+c, & otherwise.\end{cases} \qquad (22)$$

The spatial wave (hole-effect) variogram model

$$\gamma(h;\theta)=c_0+c(1-(r/h)\sin(h/r)). \qquad (23)$$

The spatial Gaussian variogram model

$$\gamma(h;\theta)=c_0+c(1-\exp(-h^2/r^2)). \qquad (24)$$

The spatial Mat´ern variogram model

$$\gamma(h;\theta,\kappa)=c_0+c\left[1-\frac{1}{2^{\kappa-1}\Gamma(\kappa)}\left(\frac{h}{r}\right)^{\kappa}J_\kappa\left(\frac{h}{r}\right)\right], \qquad (25)$$

where $J_\kappa(.)$ is the modified Bessel function of second kind of order κ, and is κ a parameter controlling the smoothness of the realized random field (Mat´ern, 1986).

Note that the temporal variogram models are defined exactly in the same way that we defined the spatial variogram models by replacing h by t.

[4] Although, the definition of the variogram indicates that $\gamma(0)=0,\hat{\gamma}(0)\neq 0$ due to the high variability between the observations taken at two very close points which leads to increase the size of the discontinuity at zero. The discontinuity of the variogram at zero is called a *nugget* effect.

[5] It is very often that the variogram stops increasing beyond a certain distance and becomes more or less stable around a limit value called a *sill* value.

[6] The correlation between two variables tends to be equal to zero when the distance h becomes too large. The distance r beyond which $C(h)$ can be considered to be equal to zero is called the *range*.

2. Study area and dataset:

Gaza Strip is a small region with a total area of 365 kilometers located in arid and semi-arid areas on the eastern coast of the Mediterranean Sea at longitudes $34^{o}200''$ East and latitudes $31^{o}250''$North. It is well known that the Gaza Strip is one of the world's most densely populated areas and its main aquifer is not complying with the population needs. The irrigation and drinking water quality in Gaza Strip are not complying with World Health Organization (WHO) standards due to the contamination resulted from the sea water intrusion (Shomer et al., 2004, Al-Najar, 2011). This intrusion is seriously affecting the quality of the groundwater where the chemical and statistical analysis of the wells indicate high salinity, high nitrate and chloride concentration and high sodium adsorption ratio (SAR) ratio (Shomer et al., 2004, Al-Najar, 2011, and Mahdi 2016). It is expected that the sea water intrusion will be increased in the coming few years.

In general, irrigation water quality is judged by some determining factors such as Sodium Adsorption Ratio (SAR), Soluble Sodium Percentage (SSP), Residual Sodium Carbonate (RSC), and Electrical Conductance (EC) (Richards, 1954).

The higher the sodium adsorption ratio is, the less suitable the water is for irrigation so that the SAR is considered to be the most commonly method used to predict a potential the infiltration problem[7]. The SAR procedure encompasses the infiltration problems due to an excess of sodium in relation to calcium and magnesium that is given from the equation

$$SAR = \frac{Na^{+}}{\sqrt{\frac{Ca^{2+}+Mg^{2+}}{2}}}, \qquad (26)$$

where Na^{+}, Ca^{2+}, and $Mg^{2+}$are the Sodium, Calcium, and Magnesium respectively measured in milliequivalents/liter.

On the basis of SAR, the sodicity hazard of the irrigation water have been divided into four categories given in Table 1 below

Table 1 *Sodicity hazard of irrigation waters.*

SAR, me/l	Sodicity class	Sodicity hazard
<10	S1	Low
10-18	S2	Medium
18-26	S3	High
>26	S4	Very high

Source: (Richards 1954).

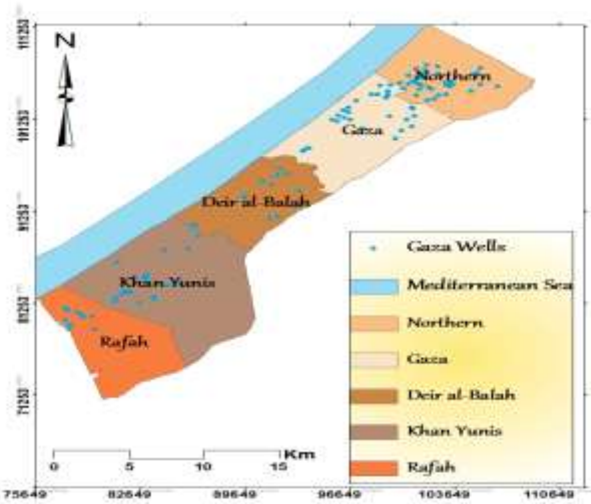

Figure 1: Distribution of groundwater wells in Gaza Strip (365 km^{2}).

There are more than 4000 wells within the Gaza Strip. More than 97% of these are privately owned, where they have been exploited in an irrational unmanageably usage for agricultural purposes. As of 2009, only 109 wells are operated by the municipalities[8] where they are mainly used for domestic supply of drinking water. Figure 1 shows the distribution of the groundwater wells in the study area throughout the Gaza Strip. The target variable is the Sodium Adsorption Ratio (SAR) in drinking water wells, where we have 109 observations recorded annually in the spring seasons for the period 2001 to 2009 on spatial locations $77585.36 \leq X \leq 106475.1$ and $78491.00 \leq Y \leq 107217.9$.

3. Geostatistical results:

[7] An infiltration problem occurs if the irrigation water does not enter the soil rapidly enough during a normal irrigation cycle to replenish the soil with water needed by the crop before the next irrigation.

[8] There are 25 municipalities distributed in the five governorates of the Gaza Strip: Northern, Gaza, Deir el-Balah, Khan Yunis, and Rafah governorates.

In this section, we report the geostatistical results obtained from the analysis of the SAR values in the irrigation and drinking groundwater dataset throughout Gaza Strip. We use **R** and **ArcMap GIS** software to analyze the SAR data. Table 2 shows the summary of the statistical evaluation of the SAR values in the groundwater dataset. The range of the SAR values was from 0.17 to 21.7, where the highest SAR value related to Khan Yunis governate and the lowest value related to Northern governate.

Table 2 Descriptive statistics of SAR values

Year	Min	Max	Mean	St. Dev.
2001	0.9	21.2	5.6	4.9
2002	0.2	18.7	4.5	3.9
2003	0.8	18.2	5.7	3.9
2004	0.6	18.1	6.8	3.9
2005	0.3	21.7	5.9	5.0
2007	0.4	12.4	4.8	2.9
2008	1.6	18.0	6.3	2.9
2009	0.7	20.7	6.6	5.0

Source: Analysis of SAR values in groundwater wells throughout Gaza Strip

We apply the Kriging method described before to estimate the SAR values. First, we model the spatio-temporal correlation among the SAR values by estimating both empirical variograms (the spatial and the temporal) as well as by fitting the theoretical appropriate models to these empirical variograms.

In our analysis, the common semivariogram models (circular, spherical, exponential, Gaussian, wave, and Mat´ern) were used to describe the spatio-temporal correlation in the SAR data. After evaluating these different variogram models using cross validation method, we conclude that the exponential models (spatial and temporal) are best suited for both corresponding empirical variograms, so that they were selected as best fitted models describing the spatio-temporal correlation in the SAR data. Figures 2 and 3 show the estimated variograms whereas Table 3 summarizes the parameter estimates of the exponential fitted variogram models:

$$\gamma_s(h) = 5.92 + 23.22(1 - \exp(-3h/122)) \quad (27)$$

and

$$\gamma_t(t) = 0.52 + 2.50(1 - \exp(-3t/12.18)) \quad (28)$$

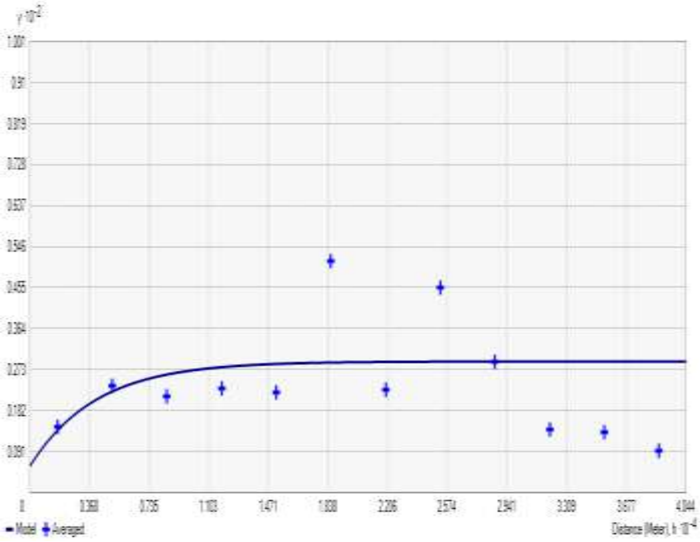

Figure 2: Empirical (+) and fitted exponential (-) spatial variogram models of SAR.

Table 3 Variogram Parameters of Exponential Model Fitted to SAR Values in Water Samples

Model	Nugget	Partial Sill	Range
Spatial	5.9173	23.221	12187
Temporal	0.52	2.50	12.18

Source: Analysis of SAR values in groundwater wells throughout Gaza Strip throughout Gaza

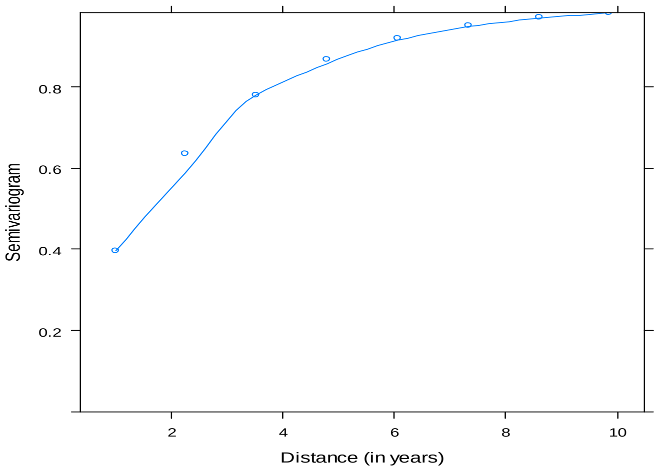

Figure 3: Empirical (∘) and fitted exponential (-) temporal variogram models of SAR.

Finally, the ordinary kriging has been applied in the space-time domain in order to estimate the SAR values in the groundwater data throughout Gaza Strip. The separable space-time variogram model given in Equation 6 is used based on the results from Table 3 and Equations 27, 28.

$$\gamma_{prod}(h,t) = C_{prod}[\gamma_s(h) + \gamma_t(t) - \gamma_s(h)\gamma_t(t)]$$

where C_{prod} is the global sill estimated to be 328.26.

Here we report the results of the first and the last years (2001 and 2009 respectively) of the dataset being analyzed. The interpolation of SAR values presented in Figures 4 and 5 here were obtained for the first and last years of the dataset being analyzed.

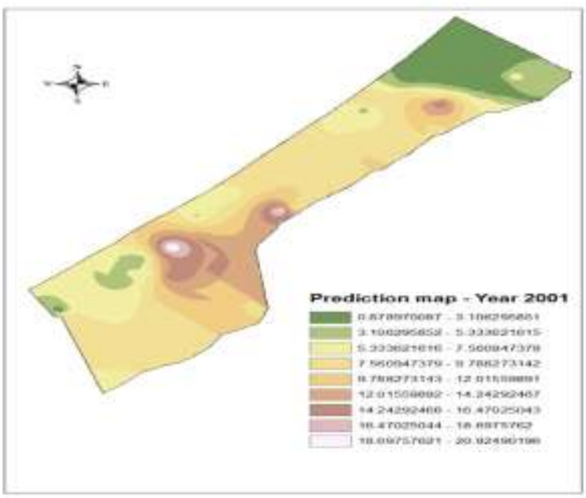

Figure 4: The interpolation of SAR values using an exponential model for the year 2001.

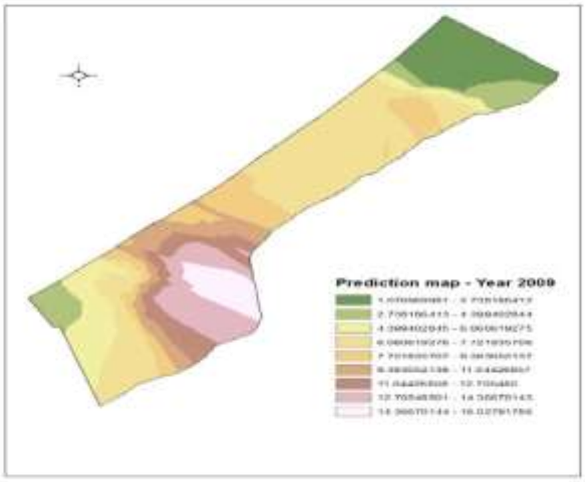

Figure 5: The interpolation of SAR values using an exponential model for the year 2009.

Visual inspection of the output maps in Figures 4 and 5 indicates a deterioration in the quality of the groundwater due to the increasing level in the SAR values over the years especially throughout the middle and south governorates of Gaza Strip.

4. Conclusion:

The present paper proposes a spatio-temporal model to map the SAR values in the groundwater as a first step to assess the suitability for irrigation and drinking purposes in the Gaza Strip area.

The ordinary Kriging method was used for the preparation of thematic maps of groundwater quality parameters of the sodium adsorption ratio. The exponential semivariogram model was best fitted for SAR values in both space and time domain.

The present study demonstrates high efficiency for using the spatio-temporal model to analyze the SAR data. Water samples analyses revealed a deterioration in the quality of the groundwater due to the increasing level in the SAR values over the years especially throughout the middle and southern governorates of the Gaza Strip.

The SAR prediction maps produced as a result of this research should be taken into account by decision-makers for sustainable land-use management in the Gaza Strip. Water managers and policymakers must start considering the excess of the SAR values in irrigation water as a serious threat to the water resources in the region.

Acknowledgments:

The author would like to extend his gratitude and appreciation to Dr. Hosam Al-Najar, Associate Professor of environmental engineering at the Islamic University-Gaza in Palestine and Eng. Ayat A. Mahdi, M.Sc. of environmental and water science at Al-Azhar University-Gaza in Palestine for providing the historical data and constructive efforts on spatial maps preparation. The author also thanks the Editor and the two anonymous referees for helpful comments.

5. Referencing:

Al-Najar H (2011). The integration of FAO-CropWat model and GIS techniques for estimating irrigation water requirement and its application in the Gaza strip. *Natural Resources 2*, 146-154.

Bilonick RA (1988). Monthly hydrogen ion deposition maps for the northeastern U.S. from July 1982 to September 1984. *Atmospheric Environment (1967)*, 22(9), 1909-1924.

Cesare LD, Myers D, Posa D (1997). Spatial temporal modeling of SO_2 in the Milan district. *Kluwer Academic Publishers*, 2(96), 1031-1042. In: Baafi, E.Y., Schofield, N.A. (Eds.), Geostatistics Wollongong.

Cesare LD, Myers D, Posa D (2001). Estimating and modeling space-time correlation structures. *Statistics & Probability Letters*, 51(1), 9-14.

Cressie N (1993). *Statistics for spatial data*. Revised edition. John Wiley and Sons, Inc., New York.

Dimitrakopoulos R, Luo X (1994). Spatiotemporal modelling: covariances and ordinary kriging systems. *Kluwer Academic Publishers, Dordrecht*, 2(96), 88-93. Geostatistics for the next century.

Dunn MR (1983). A Simple sufficient condition for a variogram model to yield positive variances under restrictions. *Mathematical Geology*, 15(4), 553-564.

Iaco SD, Myers D, Posa D (2001). Space-time analysis using a general product-sum model. *Statistics & Probability Letters*, 52(1), 21-28.

Isaaks EH, Srivastava RM (1989). *An introduction to applied geostatistics*. Oxford University Press, New York.

Jones RH, Zhang Y (1997). *Models for continuous stationary space-time processes. In Modelling Longitudinal and Spatially Correlated Data*, volume 159. Lecture Notes in Statistics. Springer, New York.

Liu X, Wu J, Xu J (2005). Characterizing the risk assessment of heavy metals and sampling uncertainty analysis in paddy field by geostatistics and GIS. *Environmental Pollution*, 141, 257-264.

Mahdi E. (January 15, 2016, submitted). *A performance comparison between empirical variograms in achieving the best valid variogram.*

Mat´ern, B. (1960; reprinted 1986). *Spatial Variation* (2nd ed.). Berlin: Springer-Verlag.

Matheron G (1962). *Trait'e de g'eostatistique appliqu'ee, Tome I, Memoires du Bureau de Recherches Geologiques et Minieres*, volume 14. Editions Technip, Paris.

Matheron G (1963a). Principles of geostatistics. *Economic Geology*, 58, 1246-1266.

Matheron G (1963b). *Trait'e de g'eostatistique appliqu'ee, Tome II, Le Krigeage. Memoires du Bureau de Recherches Geologiques et Minieres*, volume 24. Editions Bureau de Recherches Geologiques et Minieres, Paris.

Moasheri S. A. and Honarbakhsh A. and Farsani P. A. (2013). Estimation spatial distribution of sodium adsorption ratio (SAR) in groundwater's using ANN and geo statistics methods, the case of Birjand plain, Iran. *International Journal of Agriculture: Research and Review*. ol. 3 No. 4 pp. 908-916.

Myers D, Journel A (1990). Variograms with zonal anisotropies and non-invertible kriging systems. *Mathematical Geology*, 22, 779-785.

Omran El-Sayed (2012). A Proposed Model to Assess and Map Irrigation Water Well Suitability Using Geospatial Analysis. *Water,* 4, 545-567.

Pozdnyakova L, Zhang R (1999). Geostatistical analyses of soil salinity in a large field. *Precision Agriculture*, 1(2), 153-165.

Richards L. A. (1954). Diagnosis and improvement of saline and alkali soils. *U.S. Department of Agriculture.* Agriculture Handbook No. 60: Issued February.

Rouhani S, Hall T (1989). Space-time kriging of groundwater data. *Kluwer Academic Publishers, Dordrecht*, 2, 639-651. In: Armstrong, M. (Ed.), Geostatistics.

Rouhani S, Myers D (1990). Problems in space-time kriging of hydrogeological data. *Mathematical Geology*, 22, 611-623.

Shomer B, Mueller G, Yahya A (2004). Potential use of treated wastewater and sludge in agricultural sector of the Gaza Strip. *Clean Technologies and Environmental Policy*, 6(2), 128-137.

Wikle CK (2003). Hierarchical models in environmental science. *International Statistical Review*, 71, 181-199.